Effect of Heat Treatment of a Melt on the Structure and Properties of the Corresponding Crystalline Ingots or Castings

P. Popel', V. Sidorov, I. Brodova, M. Calvo-Dahlborg, U. Dahlborg

Effect of Heat Treatment of a Melt on the Structure and Properties of the Corresponding Crystalline Ingots or Castings

P. S. Popel'[a, *], V. E. Sidorov[a, b], I. G. Brodova[c], M. Calvo-Dahlborg[d], and U. Dahlborg[d]

[a] *Ural State Pedagogical University, Yekaterinburg, Russia*

[b] *Ural Federal University, Yekaterinburg, Russia*

[c] *Institute of Metal Physics, Ural Branch, Russian Academy of Sciences, Yekaterinburg, Russia*

[d] *University of Rouen, Rouen, France*

**e-mail: pspopel@mail.ru*

Received June 21, 2019; revised August 12, 2019; accepted September 14, 2019

Abstract—The modern concepts of the structure of liquid metals and alloys are considered. Several types of microinhomogeneity and microheterogeneity are shown to exist in liquid metal solutions. Their structural state changes as a result of variations in composition, history, temperature, and pressure or the influence of various external actions. Upon subsequent cooling at an appropriate rate, these changes can persist up to liquidus and affect the structure and properties of the solidified alloy. The main attention is paid to the influence of the heating temperature of a liquid metal. For aluminum-based alloys, the possibility of developing the optimum heat-treatment conditions for melting using the results of studying the structure and properties of melts has been shown. This optimized heat treatment of melts is shown to be an effective method to improve the quality of alloys.

Keywords: melts, microinhomogeneity, microheterogeneity, structural transformations, overheating, aluminum alloys

INTRODUCTION

Most technological processes for the production of metallic alloys include the transformation of charge materials into a molten state and the subsequent solidification of the system at various, sometimes very high, cooling rates. When trying to improve the structure and service properties of ingots, castings, and deformed semifinished products, technologists paid great attention to the search for optimal solidification conditions. Only the first stage of this process, an initial melt, traditionally remained beyond the interests of metallurgists. In most cases, attempts to influence a system at this stage consisted in additional alloying to optimize its composition or in refining to remove harmful impurities.

However, a large body of data, which indicated that metal melts are very complex dynamic systems, has been accumulated in the last 50–60 years in scientific journals. They can exist in various structural states and pass from one state to another under the influence of various external influences. The role of the structural state of an initial melt in the formation of the structure and properties of the ingots formed from this melt and, then, in the structure and properties of deformed semifinished products was established. As applied to steels, cast irons, and some nickel alloys, these facts were systematized in monograph [1] published in 1984 and monograph [2]. The authors of [3] summarized their data on the influence of processing of a liquid metal in the production of aluminum alloys. A brief review of the effect of heat treatment of melts on the properties of amorphous materials was made in [4].

In this article, we consider the effect of heat treatment of initial melts on the structure and properties of the corresponding crystalline metal alloys. There are several types of microinhomogeneity and microheterogeneity of liquid metal solutions. Their structure depends on the composition, the temperature, and the history. This structure can be modified using temperature and pressure variations and other physical actions. At a proper cooling rate, changes in the structure of the melt can be retained down to liquidus and the effect of action on the structure and properties of a solidified alloy can also be retained. The efficiency of optimized heat treatment of a melt as the simplest external action on a liquid–metal system will be shown. In addition, we summarize the results of applying this action in the production of aluminum alloys in traditional metallurgical processes, which are characterized by moderate cooling rates ($1–10^3$ K/s).

MICROINHOMOGENEITY AND MICROHETEROGENEITY OF LIQUID ALLOYS

Short-Range Order and Structural Transformations in Liquids

The strong interaction of particles in molten metals and alloys significantly limits their relative position: the resulting correlation is called a local or short-range order. The nature of this ordering and the size of clusters with strongly correlated particle positions depend on the composition of the material, temperature, and pressure. The atomic ordering in small clusters of simple substances with a close packing of atoms is often interpreted as fragments of a hexagonal close packing, the cubic face-centered lattice, or icosahedra [5]. This local order can be characterized by geometric parameters, which are invariant with respect to rotation (e.g., coordination distances and numbers, characteristic angles in scattering curves). To take into account the restrictions imposed on the relative positions of particles by a local order, a system is described in terms of local (short-range) order parameters.

Metal melts are systems with a strong interaction of particles. Therefore, the short-range order in them is thought to be close to a crystalline order. We assume that the local order in such systems is preserved due to strong interactions at short distances and changes insignificantly even after global ordering is destroyed in melting. The latter phenomenon is described as the growth of topological defects with the density that is low enough to identify a local structure [6, 7]. In terms of local order, local symmetry axis fluctuations with the loss of axis correlation at a certain finite distance are allowed. In the presence of only one type of short-range ordering, this leads to the orientational model of melting [8, 9].

The interaction of atoms in a one-component substance can cause an additional type of local order. The competition between various types of short-range order in a solid body leads to polymorphic phase transitions. Following this idea, the authors of [10] formulated a schematic model for a substance with a Hamiltonian written in terms of the local crystalline states of clusters and orientations in the arrangement of these clusters and studied phase transitions in this model. If an additional type of local order can be formed as a result of polymorphic transformation of a substance, this model predicts the existence of polymorphic structural transitions in melts. Son and Rusakov [11] applied the theory of local states proposed in [6] to pure liquid metals with various types of local ordering and showed the existence of the temperatures and the pressures at which the probabilities of ordered states change dramatically. Studying the behavior of free energy near these points, they classified these transformations in a liquid metal as first-order phase transitions.

Iron is the most abundant metal, which exhibits polymorphic phase transitions near the melting point and strong local ordering. Therefore, it is natural to assume that polymorphic phase transitions can take place in the molten state of iron and the related systems.

Indeed, many anomalies were detected in the property–temperature relations of liquid iron in the temperature range 1640–1680°C, and they can be interpreted as indirect evidence of local order transformations [12]. Some authors associated these effects with sharp changes in the impurity content. However, during measurements of the magnetic susceptibility χ of liquid iron, Sidorov [13] showed that the anomaly the form of a jump on a $\chi(T)$ curve is more pronounced when the impurity content is a sample decreases. Therefore, this anomaly is associated with a change in the local order of liquid iron rather than with impurities. The X-ray diffraction experiments [14] showed that the characteristic interatomic distances and coordination numbers of liquid iron below anomaly temperature T_{an} corresponded to the δ structure of the initial crystal and that this structure became a γ-like one at $T > T_{an}$.

At least two types of local order usually take place in a crystalline two-component alloy with limited miscibility of the components, and each of them corresponds to a phase where one of the components is predominant. For two types of local order caused by two components in a system, two different phase transitions were shown to take place in the model [10]: an orientational order–disorder transition identified as melting and a phase transition between phases with different component concentrations. The latter transition takes place both in crystalline and molten states. The phase diagram of this model is likely to coincide with the well-known diagrams containing eutectic and monotectic equilibria.

With the theory of local states in binary solutions [10], Son and Rusakov suggested the existence of fcc-, bcc-, and cementite-like local orders in the Fe–C melts and calculated all well-known phase diagram lines of this system using only a few known points (Fig. 1). The most interesting fact is as follows: this model predicts the possibility of extending the line of the δ–γ phase transition to the liquid state region, where this line disappears at a critical point. The circles in Fig. 1 illustrate the positions of magnetic susceptibility anomaly [13]. They are very close to the calculated equilibrium curve extrapolated to the liquid state region.

Therefore, the structure of binary and multicomponent liquid alloys can be considered as a mixture of clusters based on various atoms immersed in a predominant liquid component. For example, the structure of the Fe–B melts is usually represented as boron-based clusters surrounded by a liquid iron matrix. Hence, liquid metal solutions are inhomogeneous, i.e., microinhomogeneous, on a microscopic scale.

Clusters enriched in various components do not have a clear interface with the surrounding melt: their local composition and local structure change gradually with the distance from a central atom and coincide with the composition and structure of the matrix at a distance of 1–2 nm.

Another type of possible microinhomogeneity of liquid alloys prone to amorphization was considered in [15]. The authors started from the fact that the temperature dependence of the viscosity of these melts differs significantly from the Arrhenius law. This fact can be interpreted as evidence of the growth of the structural units of a viscous flow with decreasing temperature. According to their hypothesis, this effect is associated with the formation of large-scale chains or networks of metalloid atoms linked by covalent bonds. Son and Sidorov [15] developed a unique version of the statistical theory of associated solutions, which can be applied on any scale of polymerization. Its application to a binary A_xB_{1-x} system, where A atoms can be covalently bonded, showed irregular critical behavior, which is characteristic of nonmetallic glass-forming systems. This transition was related to the transformation from the globular structure of covalent bonds to a branched one.

Thus, we conclude that there are several types of microinhomogeneity of liquid metals and alloys. The scale and type of union of atoms can be changed by changing the melt temperature or by various external actions on a melt.

Metastable Microheterogeneity

Along with the aforementioned clusters, chains, and networks, larger regions enriched in one of the components, about 10–100 nm in size, can exist in binary and multicomponent liquid metal solutions. These regions are separated from the surrounding melt by a clear interphase boundary [16]. Therefore, the system as a whole is heterogeneous on a nanometer level, or microheterogenous. The first convincing evidence of this fact was discovered in the sedimentation experiments [17]. The author noted an unusual enrichment in a heavy component of the lower part of the eutectic melts under natural gravity or their peripheral part during rotation in a centrifuge. When studying the temperature dependences of the properties and structure of the short-range order in such melts, we [18] understood that these microheterogeneous states are metastable or nonequilibrium rather than thermodynamically stable (according to the Gibbs classification, we consider metastable states as equilibrium states having limited stability in relation to external excitations and a limited lifetime). The main cause of their appearance is the initial heterogeneity of a melt caused by its history (for example, due to melting of a heterogeneous ingot with eutectic and primary crystals, heating of a stratified melt above the miscibility gap, mixing of components at the temperature

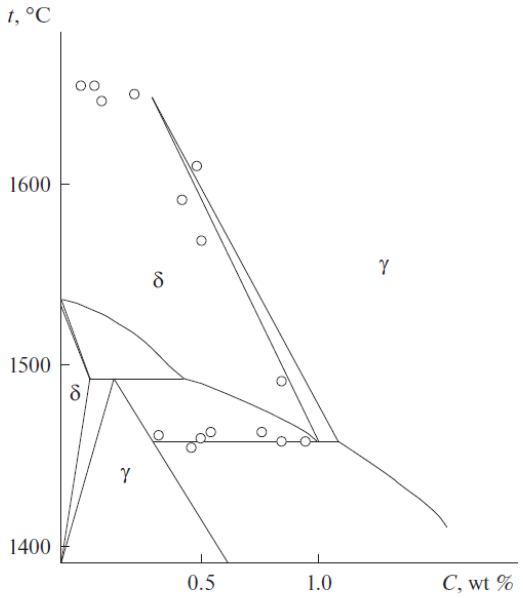

Fig. 1. Modified Fe–C phase diagram [10]. The anomalies of magnetic susceptibility determined in [13] are indicated by circles.

slightly exceeding the liquidus or miscibility gap) rather than the peculiarities of interatomic interaction. Then, the system relaxes to the thermodynamically stable state of true solution, but this process can proceed in an abnormally slow kinetic mode and can end in metastable equilibrium between dispersed particles enriched in one of the components and the surrounding melt enriched in others. The characteristic lifetime of this metastable state with small (10–50°C) overheating above liquidus is 1–10 h.

When a microheterogeneous melt is heated above a temperature determined for each composition, it irreversibly goes into the state of true solution. This phenomenon is confirmed by the branching of the temperature dependences of the properties measured during heating and subsequent cooling of samples (hysteresis of the properties). Therefore, the abscissa of the branching point can be classified as homogenization temperature T_{hom}.

As an example, Fig. 2 shows the temperature dependence of the surface tension of the Ni–B melts [19]. The melt formed after melting of an initial ingot is thought to be microheterogeneous below the branching point T_{hom}. Near T_{hom}, it irreversibly goes into the state of true solution. By plotting T_{hom} points for various compositions on the Ni–B phase diagram, we obtain a dome-shaped curve inside which metastable microheterogeneity of melts occurs (Fig. 3).

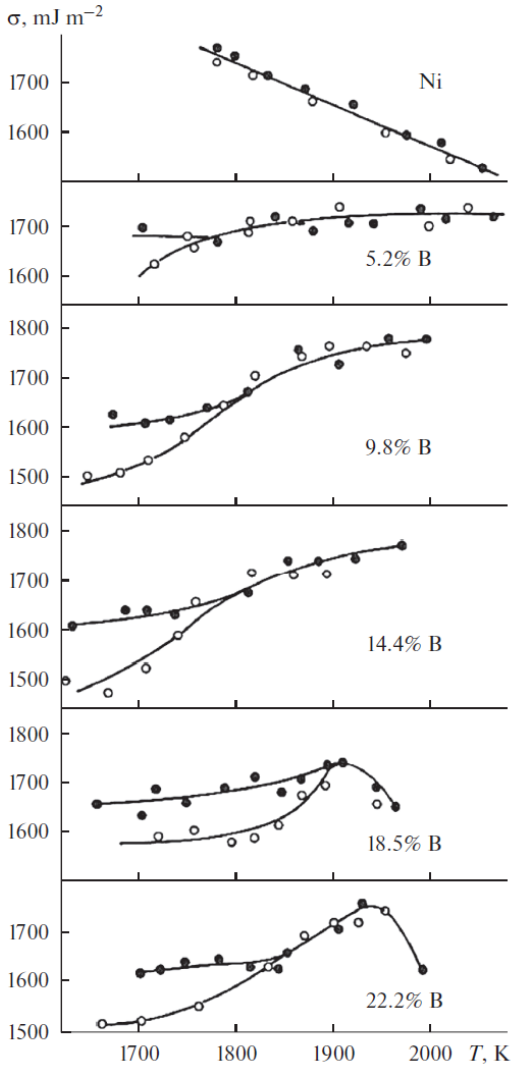

Fig. 2. Temperature dependences of the surface tension of the Ni–B melts obtained upon (●) heating after melting and (○) subsequent cooling.

Quite convincing results in favor of the metastable microheterogeneity of liquid alloys were also obtained by studying the temperature dependence of the magnetic susceptibility χ of the eutectic Au–Co melt [20]. This system is of particular interest, since its eutectic point lies somewhat lower than the Curie point T_C of cobalt-rich solid solutions. Consequently, if dispersed fragments of the initial eutectic phases are indeed preserved in this system after melting, one could expect significant magnetic effects associated with the disappearance of ferromagnetism in dispersed cobalt-based particles.

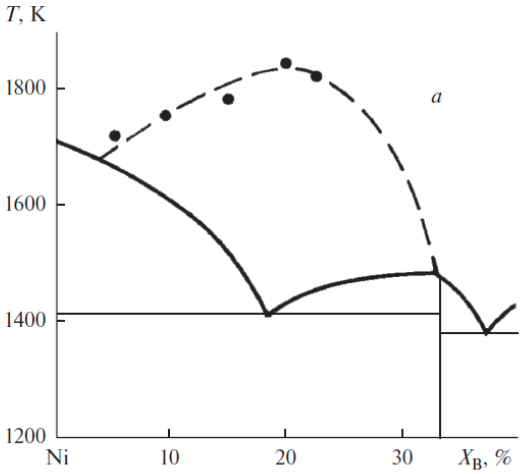

Fig. 3. Ni–B phase diagram. The dashed line above the liquidus bounds the region of metastable melt microheterogeneity.

The experimental results presented in Fig. 4 confirm this assumption: a distinct anomaly is clearly visible near the Curie temperature of cobalt-rich alloys on the $\chi(T)$ curves obtained upon heating a sample after melting. If the melt was not overheated significantly above T_C, the $\chi(T)$ dependence obtained upon its cooling reproduces the heating curve along with this anomaly. However, if the inherited microheterogeneity was destroyed upon heating to 1800°C and the system went into the state of a homogeneous solution, the temperature dependence of the susceptibility below 1400°C deviated from the heating curve and did not exhibit specific features up to the eutectic temperature.

Another important effect was clearly manifested in these experiments and was subsequently confirmed in the study of other systems: after an irreversible transition of the melt to a homogeneous state, the sample solidified at a much greater supercooling than an unhomogenized sample. The level of supercooling at the solidification front is known to be the main factor determining crystal growth and, hence, the structure and properties of the formed ingot. Therefore, homogenizing overheating of the melt should significantly affect the quality of the cast metal.

In [21], we studied the electron diffraction of the eutectic Sn–Pb alloy and found that after, melting the alloy, the maxima of the radial atomic distribution function obtained as a result of the Fourier transform of its structure factor coincided with the characteristic interatomic distances of liquid lead and tin. This finding is consistent with the idea of microheterogeneity of

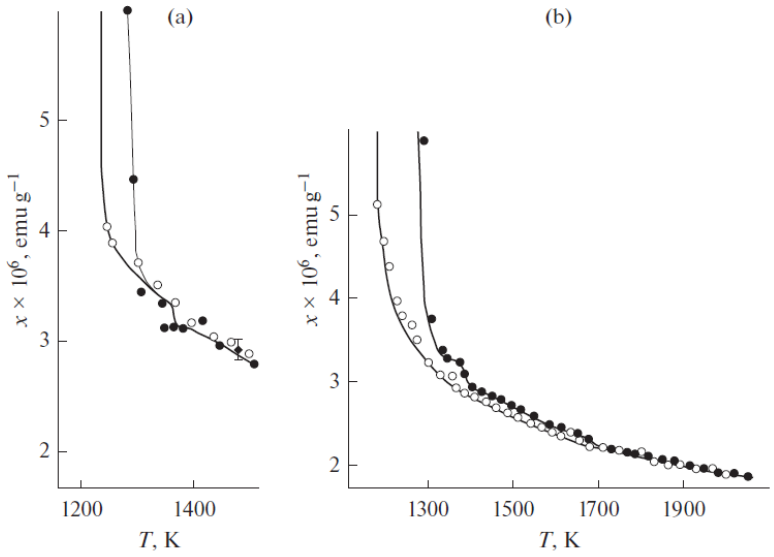

Fig. 4. Temperature dependences of the magnetic susceptibility of the Au–27 at % Co alloy obtained upon heating to (a) 1240 and (b) 1790°C (●) and (○) upon subsequent cooling [21]. The magnetic field is $H = 5.7 \times 10^5$ A m^{-1}.

the melt. At a temperature of 480°C, the maxima of both the structure factor and the distribution function significantly change their shape and position, which indicates the disappearance of microregions enriched in various components and the formation of a homogeneous solution. When the melt temperature decreases after heating above 480°C, the diffraction curves remain unchanged; i.e., a microhomogeneous state is preserved. Later [21], irreversible changes in the structure factor of this melt after heating to 650°C were recorded during its investigation by neutron diffraction.

It is interesting to note that the samples heated in a liquid state to temperatures below 430°C solidified upon subsequent cooling into a eutectic structure with a distinct triplet of diffraction rings corresponding to crystalline lead and tin. However, if the melt was heated above 480–580°C and, thus, transferred to the state of true solution, the lead reflections in the diffraction pattern of the solidifed samples disappeared, and the tin lines shifted significantly, which indicated the formation of an abnormally supersaturated solid solution of lead in tin. This final state invariably recovered after a series of successive melting–solidification cycles of this solid solution and was also retained after long-term storage of samples at room temperature. Thus, in this study, the first experimental evidence was obtained that the transition of a microheterogeneous melt into the state of a homogeneous solution (this process is called melt homogenization) is accompanied by radical changes in the structure of the solidified samples.

The first direct evidence of metastable microheterogeneity of the Sn–Pb eutectic melt was obtained when it was studied by small-angle neutron scattering (SANS) [21]. As noted above, according to densitometric data, its density upon heating exhibits anomalous behavior, which does not exist upon subsequent cooling (Fig. 5a). To understand whether this phenomenon is associated with any structural changes, neutron diffraction at 250°C was measured before and after the melt was heated to 650°C. As is seen in Fig. 5b, a distinct difference between these measurements takes place: it indicates both a change in the structure of the melt upon this heat treatment and the fact that the melt becomes more homogeneous after this treatment.

Further studies of SANS confirmed this interpretation and made it possible to obtain more detailed information about the microstructure of the melt. In particular, the particle size distribution functions obtained from these data and shown in Fig. 6 clearly indicate that the melt contains regions the atomic concentrations in which differ from the surrounding melt. These heterogeneity zones dissolve gradually upon heating to 650°C and recombine partly on subsequent cooling. As is seen in Fig. 6, regions of two different size groups are present in different amounts at all temperatures under study: one group with an average size of 1.8 ± 0.5 nm and the other group with the average size varying slightly with temperature in the range 30–90 nm.

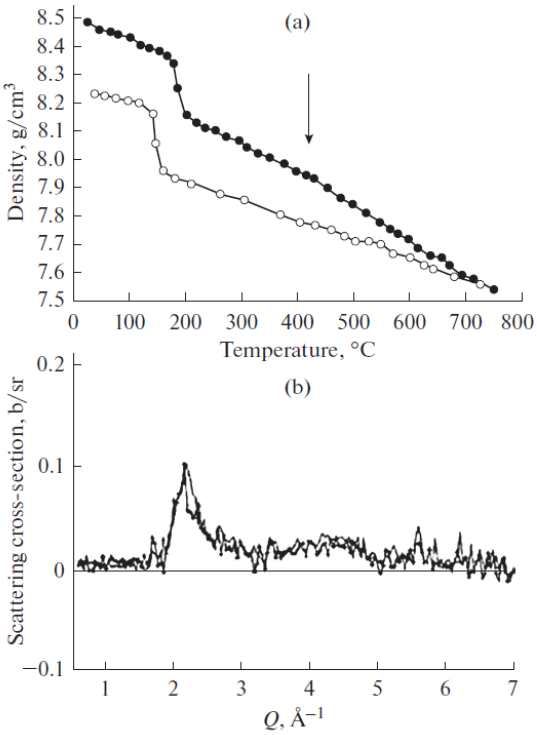

Fig. 5. Temperature dependences of the density of the eutectic Pb–Sn melt upon (●) heating and (○ subsequent cooling. (b) Difference between the static structure factors measured at 250°C before and after heating of the melt to 650°C (taken from [21]).

Sometimes, the irreversible transition of melts into the state of true solution takes place in several stages. For example, Fig. 7 shows the temperature dependence of the Ni–22.5 at % melt density [22]. After melting and isothermal holding for 5–20 h, the melt density decreases with increasing temperature. At two or three "critical" temperatures T_C, density instability appears again and the density changes in time within 5–10 h. After a new "equilibrium" density is reached, a steady linear dependence $d(T)$ is again observed during subsequent heating; however, the situation repeats itself at the next critical temperature. Only after relaxation at the last T_C, the dependence $d(T)$ becomes linear upon subsequent heating, cooling, and thermal cycling without solidification. If the sample is solidified and melted, the features detected during the first heating are again observed in the $d(T)$ curve (Fig. 7). This melt is thought to become microhomogeneous after several structural transformations of its microheterogeneous structure, which determine the instability of density at the critical temperatures. A convincing confirmation of these ideas was recently obtained when neutron diffraction was used to study the time dependences of the structure of the $Ni_{81}P_{19}$ eutectic melt [23]. This melt was held at approximately 900°C, i.e., much higher than the melting point (about 850°C), for more than three hours before recording data. The time-averaged static structure factor $S(Q)$ obtained during measurements at a temperature of 904°C for 9 h is shown in Fig. 8. This $S(Q)$ curve has the shape characteristic of a molten system, and some small peaks superimposed on a smooth curve can be seen. It can be concluded that, despite

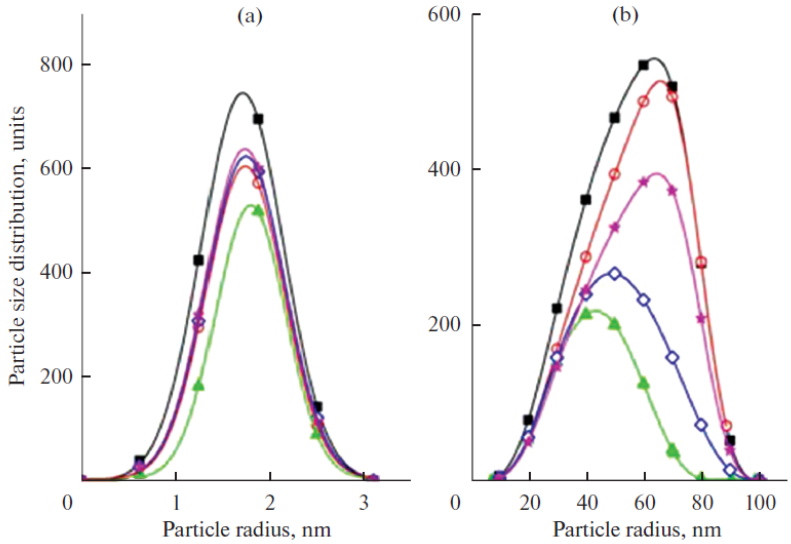

Fig. 6. Particle size distribution function for the molten eutectic Pb–Sn alloy at (■) 250, (○) 350, and (▲) 650°C upon heating and at (◇) 350 and (★) 250°C upon subsequent cooling for (a) small and (b) large atomic groups [22].

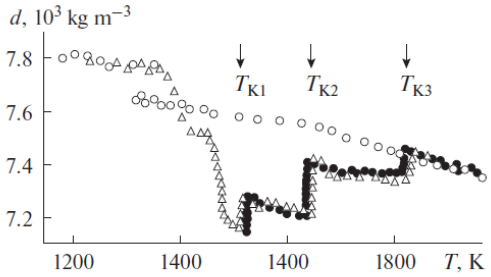

Fig. 7. Temperature dependences of the density of the Ni–22.5 at % B melt upon (●) heating after melting, (○) subsequent cooling, and (△) seconbdary heating after solidification and repeated melting [22].

long-term isothermal holding before the start of measurements, well-determined crystalline inclusions are present in the melt. The positions of the peaks observed on the curve correspond to the first five diffraction peaks of crystalline nickel; no signs of crystalline Ni_3P were observed.

The changes in the intensities of the (220) and (311) diffraction peaks of Ni, which took place during the first measurement at 904°C and the subsequent measurement at 952°C, were analyzed in more detail (Fig. 9). The measured intensities were approximated by an exponential dependence. The structural relaxation times t in both cases were found to be about four hours for the (220) peak and slightly shorter for the (311) peak. Although the approximated curves satisfactorily described the experimental data, these data, of course, can be described by other similar analytical expressions. However, this finding does not negate the fact that, obviously, nickel particles that are large enough to be detected in diffraction experiments (i.e., larger than 10 nm) exist in the Ni–P eutectic melt for several tens of hours in the temperature range 100°C wide above the eutectic temperature.

A specific type of microheterogeneity of metal melts is associated with the gas subsystem. Liquid alloys are known to contain significant amounts of gas components. For example, the hydrogen content in molten aluminum alloys substantially exceeds its maximum solubility. This means that significant part of hydrogen exists in the form of bubbles or hydrides. Using thermodynamic analysis [24], we showed that small (about 10 nm) gas bubbles can exist in stable or metastable equilibrium with the surrounding melt depending on the supersaturation, temperature T, and pressure p. Therefore, supersaturated metal melts should be considered as nanodispersed foams. When changing T and p, we can change the dispersity of the foam or transform it into the state of a true gas solution.

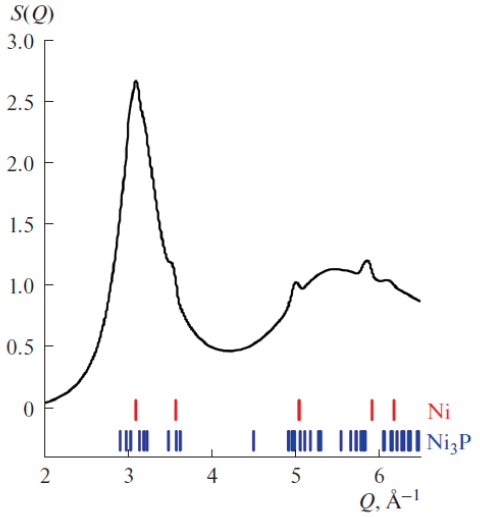

Fig. 8. Averaged statistical structure factor $S(Q)$ measured at 904°C for 8.6 h beginning from 3.1 h after the onset of the temperature cycle. The vertical lines at the bottom indicate the positions of the most intense diffraction peaks of Ni_3P taken from JCPDS.

Heat Treatment of Melt as an Advanced Method for Alloy Manufacture

Thus, we can consider the following types of microinhomogeneity and microheterogeneity of liquid metal solutions:

(i) microscopic heterogeneity, which is caused by various types of local ordering and can be changed as a result of changing the volume fraction of clusters or polymorphic changes within clusters;

(ii) medium-scale fractal heterogeneity, which is caused by the existence of two or more types of interatomic interaction and can be changed due to the evolution of metalloid chains, namely, elongation, networking, and coalescence into globules;

(iii) nanoscale metastable microheterogeneity, which is caused by the history of the melt and can be changed due to transformations of the volume fraction, the size, and the composition of dispersed particles or nanobubbles.

Considering that different types of microinhomogeneity and microheterogeneity usually coexist, we have to conclude that metal melts are very complex systems. Their structure can be changed by changing the temperature or pressure or using various external actions on it. Upon subsequent cooling at a proper rate, these changes can be retained down to the liquidus temperature and affect the structure and properties of the solidified (crystalline, nanocrystalline, amorphous) alloy. The data on structural rearrangements in metal melts presented above allow us to identify the most promising methods of external actions on

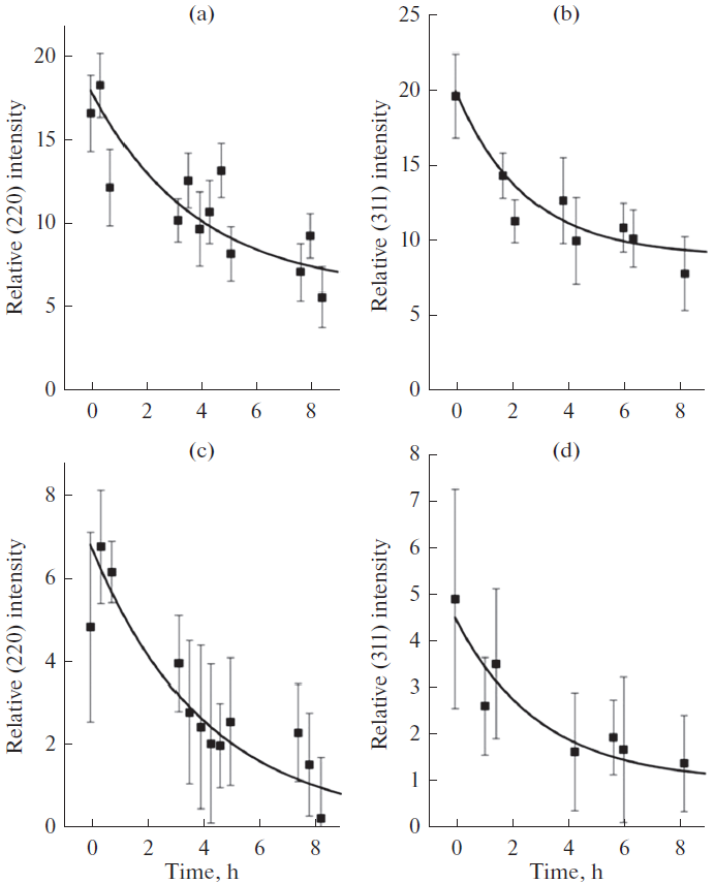

Fig. 9. Time evolution of the (220) and (311) diffraction peaks of Ni: (220) at (a) 904 and (c) 952°C and (311) at (b) 904 and (d) 952°C. The curves illustrate the exponential approximation of the experimental data.

liquid metals and alloys in order to improve the quality of cast, deformed, and rapidly quenched products made of them.

One of them is the processing of liquid alloys by powerful ultrasonic vibrations, which is accompanied by the development of acoustic cavitation and acoustic flows in the metal volume. As a result of the appearance of cavitation bubbles, their fragmentation into smaller ones, and subsequent collapse, effective melt homogenization can be achieved [3]. Of course, this processing of a melt requires rather complex equipment and can be carried out only for not too high-temperature systems.

The temperature treatment of liquid metals and alloys (overheating above liquidus to a certain temperature, isothermal holding at this temperature for a certain time, and subsequent solidification at a proper cooling rate) is though simple but no less effective. No attempts were made to apply it to pure liquid metals to initiate the phase transitions described in the works of Son et al. and to preserve a high-temperature structure upon sufficiently rapid cooling to solidification. However, it seems to be a rather promising method for improving the crystal structure of metals susceptible to such transitions.

The most radical method seems to be homogenizing heat treatment of initially microheterogeneous melts. Their overheating above the liquidus to the temperature exceeding the point of irreversible transition of a system to the state of true solution allows us to significantly affect the conditions of phase formation during solidification and the properties of solidified alloys. An increase in the maximum melting temperature without going beyond the region of metastable microheterogeneity can lead to less significant but also useful effects. The changes in the dispersion and phase composition of the microheterogeneous melt that are achieved during such processing can be retained until the beginning of solidification at sufficiently high

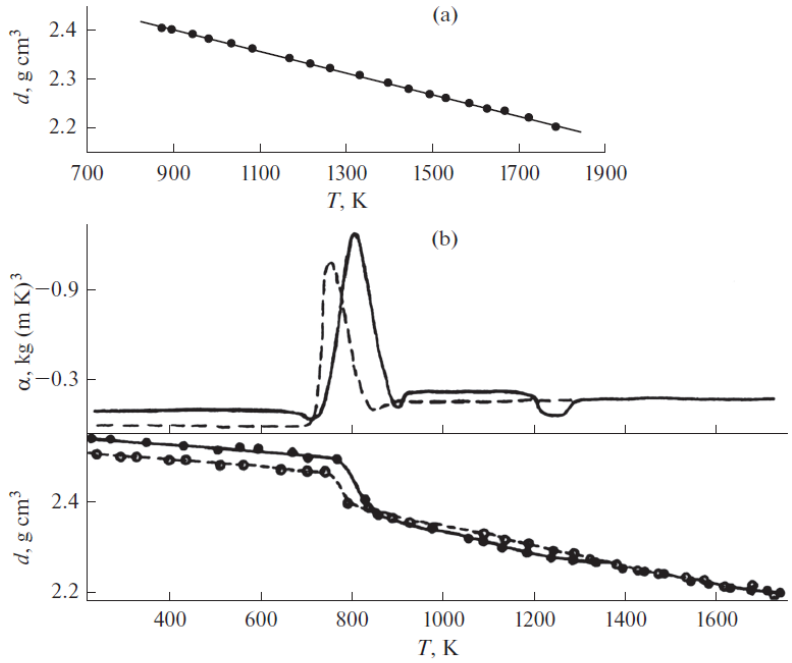

Fig. 10. (a) Temperature dependence of the density of the eutectic Al–Si melt prepared at 1450°C obtained upon cooling and (b) temperature dependences of the density and the thermal expansion coefficient of the melt sample. (●, ○) Experimental data obtained upon heating and cooling of the sample, respectively, and (lines) smoothing spline and its derivative.

cooling rates, providing modification of the cast metal.

In many cases, a significant overheating of a liquid alloy cannot be achieved under industrial conditions due to insufficient power of melting equipment, the low resistance of refractories, and other technological and economic limitations. As a result, the problem arises of lowering the melt homogenization temperature to acceptable values. This problem can be solved by introducing small amounts of impurities into a liquid alloy, which decrease the interfacial tension at the boundary of dispersed particles in a microheterogeneous melt (this tension determines the thermal stability of particles) [25]. In this case, we deal with modification of a melt structure, which can improve the quality of the cast metal.

In the following sections, we consider the results of practical application of heat treatment of liquid alloys in more detail.

EFFECT OF HOMOGENIZING HEAT TREATMENT OF MELT ON THE STRUCTURE AND PROPERTIES OF ALUMINUM ALLOY INGOTS

The study of the influence of heat treatment of an initial melt on the structure and properties of steels began in the 1970s by Baum et al. [1]. They were the first scientists to use the temperature dependence of the properties to determine the characteristic heating temperature of a liquid metal. Since these and their subsequent results are summarized in [1, 2], in this article we restrict ourselves to the results of studying the effect of heat treatment of melts on the structure and properties of aluminum-based alloys with various types of phase diagrams [3].

Aluminum Alloys with Simple Eutectic

A detailed study of the structural transformation temperatures of aluminum–silicon melts, which are the basis of industrial silumins, was begun by densitometric investigations [26]. It was shown that, if the components of a eutectic composition sample were mixed at 1450°C, no anomalies that could be associated with structural changes in the melt were detected in the temperature dependence of the density obtained upon cooling from this temperature (Fig. 10a). However, the densities detected after solidification and repeated melting of samples were approximately 1% lower than those before solidification (Fig. 10b). In the temperature range between 950 and 1110°C, the authors of [26] observed an anomalous decrease in thermal expansion coefficient α, after which the $d(T)$ curve merged with the cooling curve of the initial melt

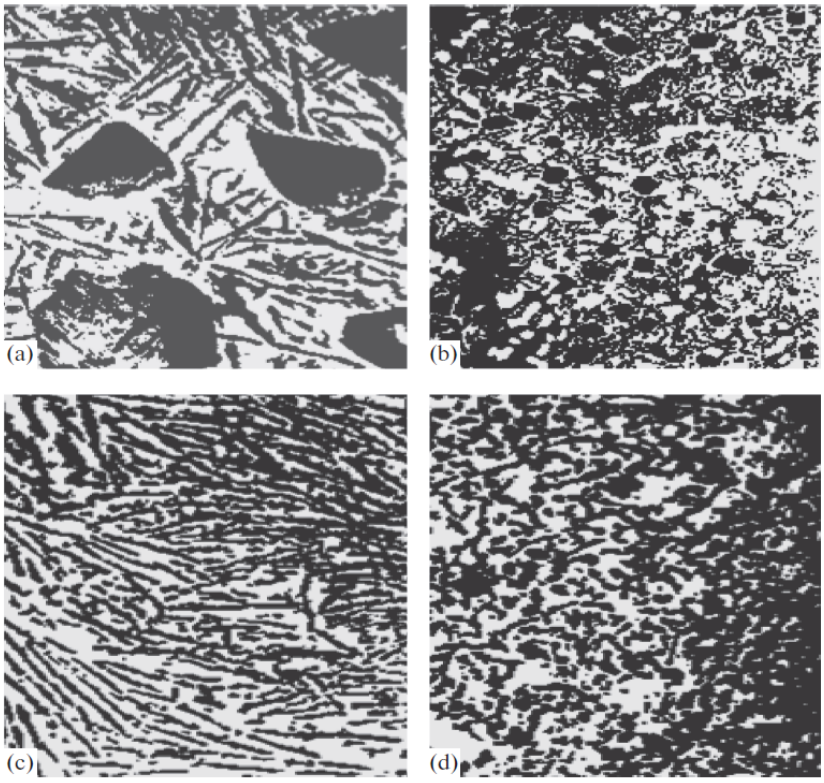

Fig. 12. Structures of the Al–17 at % Si alloy melted without homogenizing overheating and solidified at a rate of (a) 10^2 and (b) 10^5 K/s and this alloy subjected to HTT in a liquid state and solidification at a rate of (c) 10^2 and (d) 10^5 K/s (×200) [26].

First, in [31] we studied the temperature dependences of the density and the viscosity of the samples containing up to 1.5 wt % Zr and prepared from high-purity reagents (iodide Zr and Al with an impurity content of at most 0.001%). The results presented in Fig. 13a show that, in the temperature range from liquidus to 1800°C, signs of completion of the transition of the system into the state of true solution are only observed in a sample with the minimum zirconium content near 1600°C. For higher second-component concentrations, this transition is incomplete up to the highest temperature of the temperature range under study, as evidenced by the absence of coincident parts of the $d(T)$ curves recorded in heating and subsequent cooling. This conclusion was also confirmed by the results of a viscometric study, in which high-purity alloys containing up to 2 at % Zr were investigated. In the temperature range up to 1820 K, no signs of irreversible changes in the structure of the melt were found.

However, when studying the temperature dependences of the viscosity of a commercial-purity Al–2 wt % Zr master alloy, we obtained quite nontrivial results indicating the complexity of the processes accompanying an increase in the temperature of the sample. In the initial segment of the temperature dependence (approximately up to 1050°C), the viscosity increases upon heating (Fig. 13b). Then, the rate of increase of ν slows down, and, finally, a "normal" decrease in the viscosity with increasing temperature is established. This high-temperature dependence is retained upon further cooling, and, below 1200°C, the $\nu(T)$ curve deviates from the curve recorded during initial heating. As follows from these results, a commercial-purity sample reaches the state of true solution near 1230°C, i.e., at the temperature that is much lower than the homogenization point of a similar alloy melted from high-purity components. This fact was the starting point in the idea of modifying melts with specially selected additives to lower their homogenization temperature.

To study the effects of heat treatment and the melt cooling rate on the structure of Al–Zr alloys, we studied samples of hyperperitectic compositions containing 0.6, 1.5, 2.0, 3.0, and 4.7 wt % Zr. It was found that, at a low melt overheating ($\Delta T < 150$ K) and low cooling rates, the Al_3Zr intermetallic compound with the tetragonal crystal lattice of space group $D0_{23}$

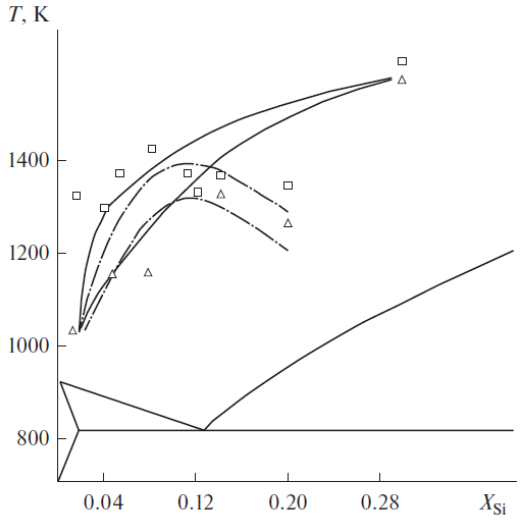

Fig. 11. Decomposition dome of the metastable microheterogeneity in Al–Si melts plotted using the temperature dependences of (-·-·-) density, (△) kinematic viscosity, and (□) electrical resistivity ρ.

and did not have any further specific features for any temperature variations in the range from the eutectic temperature up to 1450°C. Similar anomalies, but at slightly different temperatures, were also observed for samples the compositions of which differed from the eutectic composition.

A difference between the property–temperature curves obtained upon heating of hypo- and hypereutectic Al–Si melts to 1200–1400°C was also revealed by studying their viscosity ν [27]. Interestingly, in the temperature range below the branching point, the heating curves ν(T) of hypoeutectic compositions are above the cooling curves. After passing the eutectic concentration, inversed viscosity hysteresis is observed: the viscosity upon cooling exceeds the viscosity upon heating.

These results were interpreted by the authors using the concept of hereditary metastable microheterogeneity of liquid eutectic alloys; i.e., the anomalies of the $d(T)$ and ν(T) curves were explained by the irreversible transitions of the microheterogeneous melt formed after melting into the state of true solution. Having plotted the points of the density and viscosity anomalies on the Al–Si phase diagram, we determined the temperature–concentration boundaries of the region in which microheterogeneous states of liquid silumins take place (Fig. 11). The absence of branching of the temperature dependences of viscosity for a eutectic composition sample allowed the conclusion that the irreversible viscosity changes are associated primarily with the destruction of the dispersed particles formed from the fragments of the primary phase in an initial ingot. The composition of this phase changes when passing through the eutectic point, which leads to an inversed viscosity hysteresis.

To study the effect of homogenizing heat treatment (HHT) of a melt on the structure of solidified samples at various cooling rates, we [3] used the generally accepted procedures for quenching from a liquid state, which make it possible to heat a melt to high temperatures and to cool it at rates in the range 10^2–10^6 K/s with parallel temperature control in most cases.

These experiments were carried out with a hypereutectic silumin containing 17 wt % Si [26]. The experimental data characterizing the structural state of this melt clearly indicate that, after melting, it is microheterogenous; therefore, there are prerequisites for controlling its structure by HHT. Alloy Al–17Si (wt %) samples were prepared using various technologies: by casting in a graphite mold (V < 100 K/s) and melt quenching (V = 10^2–10^4 K/s). The overheating temperature range was 100–500°C.

Figure 12 shows the structures that were fixed after solidification at various rates of the melt subjected to HHT on heating above liquidus to 1200°C and without this treatment. A comparison of these structures shows that, after HHT, primary silicon crystals disappear in the structure of the solidified metal and the entire structure becomes quasi-eutectic, although the silicon concentration in it exceeds the eutectic concentration by 5% (Figs. 12c, 12d). If the cooling rate is increased to 10^6 K/s, primary α solid solution dendrites are clearly visible against the background of globular eutectic in the structure of crystalline samples after homogenizing overheating of the melt; that is, the hypereutectic alloy begins to solidify as a hypoeutectic one.

Therefore, HHT of the melt can be considered as the cause of a deep supercooling at the solidification front, and, after its application, the stable phase diagram of the alloy changes into a metastable diagram even at ordinary solidification rates. A combination of high cooling rates and HHT leads to a further change in the phase diagram, namely, to the appearance of primary α solid solution crystals in alloys with an initially hypereutectic composition.

Aluminum Alloys with Compounds

The influence of heat treatment of initial melts and the cooling rate on the structure of ingots was studied for many aluminum-based alloys with compounds (Al–Zr, Al–Ti, Al–Mn, Al–Mg, Al–Sc, etc.) [3]. The Al–Cu system was recently studied in most detail [28–30].

We now consider typical effects using Al–Zr alloys as an example. This system was the first for which the characteristic temperatures of structural transformations in a liquid state were determined.

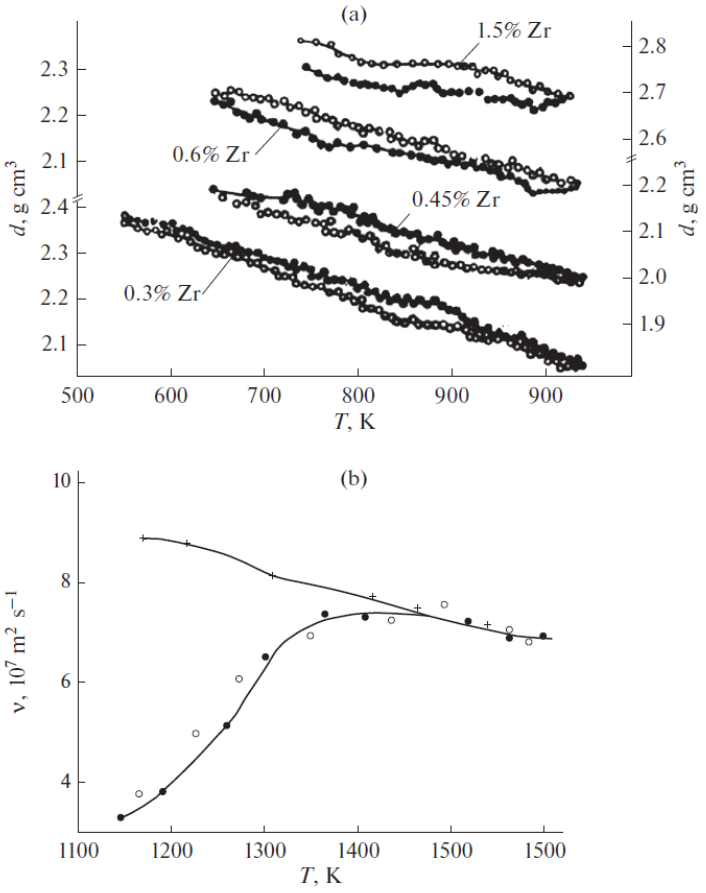

Fig. 13. (a) Temperature dependences of Al–Zr melts ((○) heating and (●) cooling; zirconium concentration is in at %). (b) Temperature dependences of an Al–2 wt % Zr master alloy ((●) primary heating, (+) cooling, (○) repeated heating after solidification).

formed in a casting in accordance with the equilibrium phase diagram regardless of the second-component concentration. The most typical shape of growth of its crystals is faceted elongated plates (Fig. 14a), the size of which decreases with increasing cooling rate. As the Zr concentration increases, the distribution of these crystals over the cross section of the sample becomes more and more nonuniform, and their average size increases from 60 to 250 μm. The intermetallic compounds of this modification grow steadily at the cooling rates lower than 10^2 K/s for Al–1.5Zr (wt %), 10^3 K/s for Al–2Zr (wt %), 10^4 K/s for Al–3Zr (wt %), and 10^5 K/s for Al–4.7Zr (wt %).

The influence of the structure of an initial melt on the size, the morphology, and the structure of the aluminide in an Al–2Zr alloy (wt %) was investigated [32, 33]. The initial liquid was overheated to various temperatures (ΔT = 100–460°C). The change in the shape of stable zirconium aluminide inclusions depending on cooling rate V and overheating ΔT above liquidus is shown in Fig. 15 (areas I, II). Fig. 14b illustrates the typical case where dendritic crystals with clear vertices of first- and second-order dendrite arms form instead of plates. Attention should be paid to the formation of much more dispersed equiaxed dendrites having a specific petal structure: their morphology and size unambiguously prove their primary origin. For each composition, there is a certain cooling rate range in which primary intermetallic compounds of a similar morphology, structure, and size form.

X-ray diffraction analysis of such crystals showed that they had the Al_3Zr composition and a cubic ordered structure, which is similar to the secondary metastable phase that nucleates during the decomposition of a supersaturated α solid solution. As the Zr concentration in the alloy increases, the conditions for

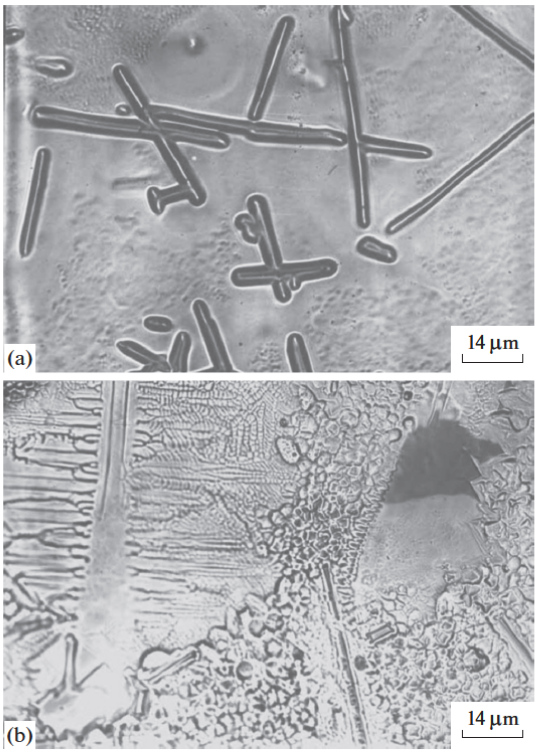

Fig. 14. Growth shapes of zirconium aluminide crystals (structure type $D0_{23}$) vs. solidification parameters for an Al–2 wt % Zr alloy: (a) $V = 10$ K/s, $\Delta T = 200$ K; (b) $V = 10^3$ K/s, $\Delta T = 360$ K.

the most stable growth of the intermetallic compounds of this metastable modification shift toward higher cooling rates. The influence of the primary overheating of a melt on the morphological stability of the growth shapes of metastable aluminides was studied. At $\Delta T = 100$°C, they were found to grow as faceted cubic crystals (Fig. 16; Fig. 15, region I'). At high ΔT, dendritic shapes become the dominant form of crystal growth (Fig. 15, region II'). At $\Delta T = 200$–250°C, the intermetallic compounds have the maximum size of 10 μm and grow as dendrites with a pronounced anisotropy of the growth rates of the primary and secondary arms (Fig. 16b). At $\Delta T = 400$°C, the crystal size decreases to 5 μm and the crystals take the shape of symmetrical dendrites (Fig. 16c). Heating above the homogenization temperature is accompanied by a sharp increase in the number of aluminides and an additional decrease in their size to 1–2 μm (shaded area in Fig. 15). Thus, changing the melt preparation conditions, we can change the size and morphology of the metastable Al_3Zr crystals over wide ranges.

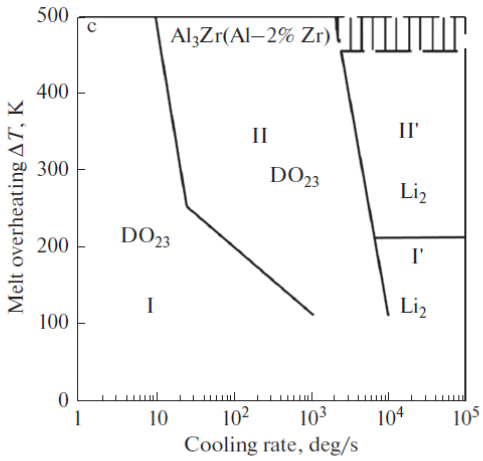

Fig. 15. Growth regions for crystals with various zirconium aluminide morphologies: (I) faceted crystals and (II) dendritic crystals.

Later, similar results were obtained for the aluminides in Al–Ti, Al–Fe, Al–Mn, and Al–Sc alloys. The following specific features were detected:

(a) The stable crystal growth shape at low cooling rates and a low melt overheating is faceted. The widest region of faceted crystals forms during the growth of scandium aluminide, and the narrowest zone corresponds to the growth of iron aluminide.

(b) When the cooling rate or the overheating of a melt increases, faceted shape changes into rounded growth shape (treelike, spherulitic, globular). Spherulitic shapes form during the solidification of the Al_3Fe and Al_6Mn aluminides, and globular shapes are found during the formation of the Al_3Sc aluminides.

(c) The overheating of a melt in combination with rapid quenching leads to the formation of metastable phases Al_3Zr, Al_3Ti and Al_6Fe.

These results correspond to the overheating of a melt to a temperature below homogenization temperature T_{hom}. Figure 17 shows the results of metallographic examination, X-ray diffraction analysis, and electron-probe microanalysis of Al–0.6Zr (wt %) alloy ribbons. The ribbons formed from the melt overheated to 1150°C were shown to have a more dispersed structure than the ribbons formed after overheating to 1220°C. Note a distinct decrease in the number of primary metastable Al_3Zr precipitates located at the centers of modified α solid solution grains and the coarsening of these grains with the casting temperature (Figs. 17a, 17b). The overheating of the melt to the temperatures close to T_{hom} changes the phase composition of the melt, and a metastable single-phase anomalously supersaturated α solid solution forms instead of a equilibrium heterogeneous two-phase

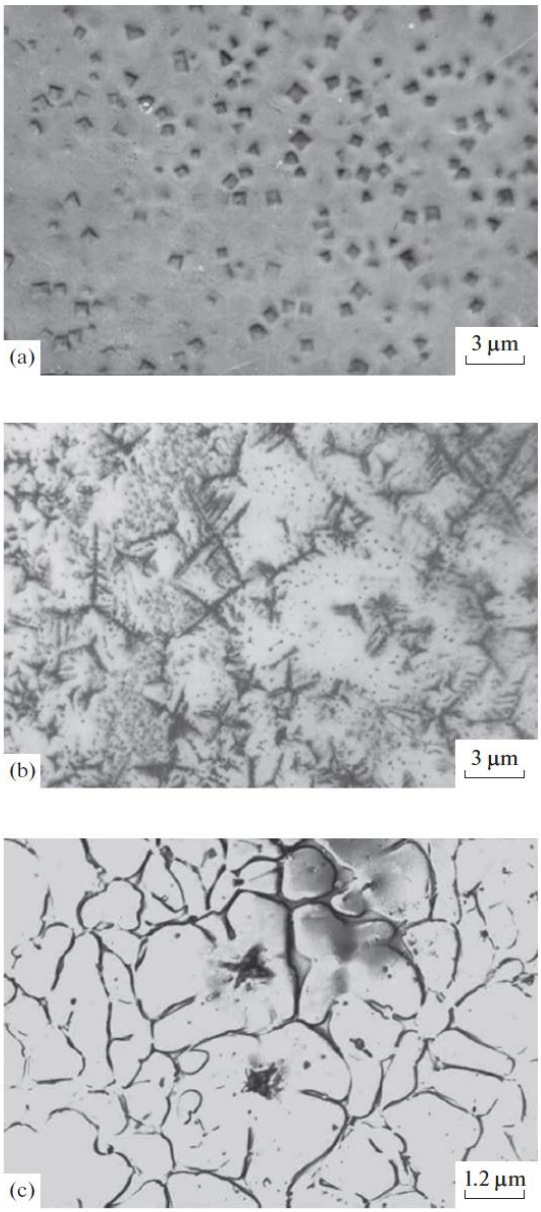

Fig. 16. Transformation of the growth shapes of zirconium aluminide crystals (structure type $L1_2$) as a function of the overheating of the initial melt ($V = 10^4$ K/s): ΔT = (a) 100, (b) 300, and (c) 450 K.

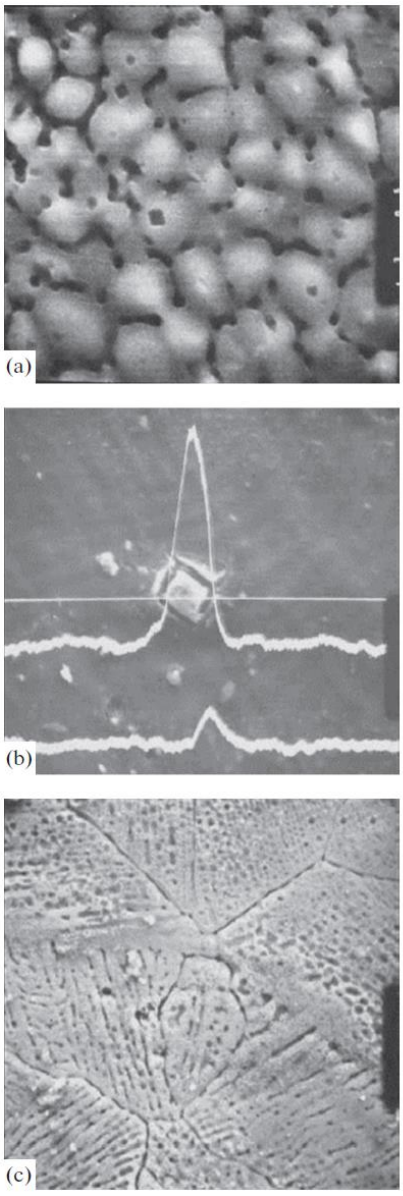

Fig. 17. Structures of alloy Al–0.6 wt % Zr ribbons formed after heat treatment of the initial melt under various conditions (backscattered electron images taken with $K\alpha$ radiation): (a, b) $T < T_{hom}$ and (c) $T > T_{hom}$.

structure (Fig. 17c). Additional holding of the melt at this temperature or cooling at a reduced casting temperature does not lead to qualitative changes in the structure of the alloy.

The positive role of HHT of a melt during the creation of single-phase structures of an anomalously saturated α solid solution with transition metals is confirmed by the results obtained in hardening an alloy

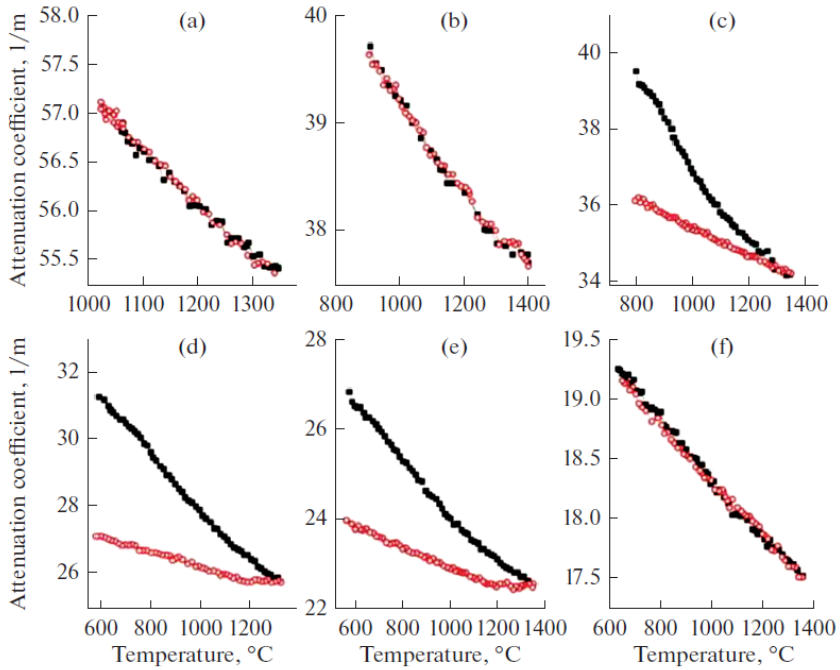

Fig. 18. Temperature dependences of the product ρμ of the following Al–Cu alloys: (a) Al_5Cu_{95}, (b) $Al_{45}Cu_{55}$, (c) $Al_{55}Cu_{45}$, (d) $Al_{75}Cu_{25}$, (e) $Al_{83}Cu_{17}$, and (f) $Al_{95}Cu_5$ upon (solid symbols) heating and (open symbols) subsequent cooling.

with a higher Zr content. For example, for an Al–2Zr alloy (wt %), such a structure forms in the ribbons formed by melt quenching at a cooling rate $V = 10^4$ K/s. However, if the melt was not subjected to preliminary HHT, the primary solidification of aluminides in the alloy is suppressed on cooling at a rate of 105 K/s.

The laws of structural changes described above were also detected during the solidification of hypereutectic Al–Ti alloys.

Thus, the use of HHT of melts during the solidification of aluminum alloys with transition metals extends the field of an anomalously supersaturated Al-based α solid solution due to the suppression of the growth of primary aluminides and the formation of a single-phase state at lower cooling rates.

As compared to the alloys with compounds described above, aluminum–copper alloys have a more complex state diagram. It has two horizontal lines corresponding to eutectic transformations and five horizontal lines with peritectic transformations. In addition, six eutectoid and seven peritectoid reactions are present. In total, this system has fifteen phases. Two of them are Cu- and Al-based solid solutions, six phases are formed with the participation of a liquid phase, and the other phases form as a result of transformations in a solid state. The authors of [29] investigated the densities of 17 Al–Cu alloys of various concentrations, most of which differed in phase compositions at the temperatures corresponding to the onset of melting. In a system with such contrasting-density components, the precipitation of dense copper-rich dispersed particles in a less dense aluminum-rich dispersion medium seems to be probable, and, vice versa, the floating of aluminum-rich particles in a copper-rich medium can be expected. In a gamma-density meter, a radiation beam passed through samples near the bottom of the crucible, where the copper concentration could significantly exceed the concentration calculated for blending. Therefore, when clarifying melts homogenization conditions, we decided to plot the temperature dependences of the product ρμ, where μ is the mass attenuation coefficient of the beam depending on the local composition of the zone to be analyzed, rather than density ρ.

The most common feature of the obtained dependences $\rho\mu(T)$ is the divergence of the heating and cooling branches (hysteresis), indicating irreversible changes in the composition and structure of the analyzed zone in most of binary melts under study after their heating above the branching point of these curves (Fig. 18). The hysteresis of the product ρμ is most pronounced for aluminum-rich samples, where the divergence of the heating and cooling branches reaches 16%. As in [28] (where branching of the temperature dependences of the viscosity of Al–Cu alloys was

noted), the authors of [29] associated this phenomenon with the irreversible destruction of the metastable microheterogeneous state of the melts inherited from heterogeneous initial crystalline samples. The anomalously large differences in the detected values of ρμ for aluminum-rich alloys can only be explained by the precipitation of dense dispersed copper-rich particles in a low-density melt.

The most unexpected result of the densitometric experiments [29] was the detection of a hysteresis in the temperature dependences ρμ(T) obtained on melting homogeneous crystalline samples of the stoichiometric compositions CuAl and (especially) $CuAl_2$. When studying the temperature dependences of the densities of molten refractory compounds (3d transition metal borides) earlier, we have not detected a similar phenomenon, and the ρ(T) curves obtained on heating and cooling of a melt coincided. We considered this fact as additional confirmation of the hereditary origin of the heterogeneity of the melts. In the case of the CuAl and $CuAl_2$ compounds, the ρμ(T) hysteresis existed, and the divergence between the heating and cooling curves was maximal at the stoichiometric concentration and decreased with the distance from it.

This phenomenon was explained in [34]. The authors believe that, on melting of relatively low-melting intermetallic compounds, like CuAl and $CuAl_2$, strong interatomic bonds, which are characteristic of the most refractory intermetallic compounds of this system (in our case, Cu_3Al), can be retained in a melt. Based on these bonds, corresponding dispersed intermetallic particles can form. However, this hypothesis needs additional confirmation.

The authors of [30] were the first to experimentally study the effect of HHT of Al–Cu melts on the structure formed after their solidification. For this purpose, they melted samples containing 10, 17.1, 25, and 32 at % Cu. One batch of samples was heated in a liquid state to 1400°C, i.e., above the temperature of their homogenization, and the second (control) batch was not subjected to this treatment. After the same melt temperature (720°C) was reached, they were solidified in a centrifugal casting machine in a bulk slot-type copper chill mold and had a disk shape 2.1–2.4 mm thick, which corresponded to the same calculated cooling rate of 6×10^3 K/s. The study of the formed crystal structures included metallographic and phase analysis and the measurement of the lattice parameter and the microhardness of the phase components.

When comparing the structures formed on quenching the samples, distinct differences in the morphologies of the crystalline phases were found. In addition, after homogenizing treatment of the melts, the solidification kinetics and, as a consequence, the phase ratio in the structure and the copper content in the phases change; the transition to metastable solidification is stimulated and the structural heterogeneity of the alloys increases

Aluminum Alloys with Monotectics

The so-called pseudo-alloys with very small and uniformly distributed inclusions of one of the components can be formed in systems with limited miscibility in a liquid state. Some of them have unique service properties (damping, tribological, etc.). The main problem of their production is associated with the tendency to macroscopic separation in cooling and significant enrichment of the lower part of the ingot with a denser component.

The macroscopic separation of such liquids is known to be suppressed when they solidify under zero gravity or in crossed electric and magnetic fields [35]. In this case, a fairly uniform component distribution over height with 1000-μm precipitates is observed. As a result of the solidification of a liquid metal at a cooling rate of 10^3–10^6 K/s, a homogeneous structure with very small inclusions can form in monotectic alloys [36]. However, such solidification conditions can be only achieved in industrial processes of formation of metal powders or thin ribbons and cannot be achieved in large-scale production of bulk castings.

Based on the positive experience obtained for eutectic alloys, Popel et al. [37] studied the possibility of suppression or deceleration of macroscopic decomposition in bulk samples of laminated aluminum alloys by heat treatment in a liquid state. Signs of the existence of colloidal microheterogeneity in these melts with a slight overheating above a macroscopic miscibility gap were noted in the ultra-acoustic and electron diffraction experiments [38] and the small-angle X-ray scattering experiments [39].

When measuring the viscosity of these melts during primary heating, the authors revealed an anomaly high scatter of its values (up to 10–15%), which was maintained up to temperatures specific for each composition. Upon further heating and subsequent cooling, stable values of viscosity were observed up to the miscibility gap boundary. The observed instability of the values of ν was thought to be due to the fact that, outside the miscibility gap, the system transforms from a macroscopically heterogeneous state into a metastable microheterogeneous microemulsion state, which, in turn, decomposes on heating to the temperatures indicated above. From here on, these temperatures are called melt homogenization temperatures T_{hom}.

By plotting the temperatures at which the viscosity stabilized on the Al–In phase diagram system, the authors obtained a dome-shaped curve that bounds the region of the metastable colloidal structure (Fig. 19). Then, the effect of HHT of melts on the

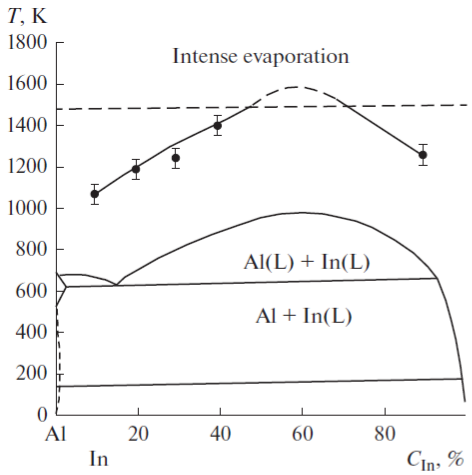

Fig. 19. Fragment of the Al–In phase diagram and the metastable microheterogeneity region.

structure formed during their solidification at moderate cooling rates (about 1 K/s) was studied on 30-g samples melted in an open resistance furnace. A clear boundary between phases enriched in various components was found to exist in solidified samples of all compositions at the temperatures of heating the melts below the microscopic separation dome shown in Fig. 19 (see Fig. 20a). X-ray diffraction analysis confirmed the separate existence of aluminum (at the top) and indium (at the bottom). When the melt temperature rises and approaches the dome-shaped separation curve, this boundary is smeared; then, at $T > T_{hom}$, the macroscopic segregation in ingots is completely suppressed. In this case, their structure becomes similar to a quasi-eutectic structure and consists of indium phase particles uniformly distributed over the aluminum matrix volume (Fig. 20b). A further increase in the melt temperature significantly affects the structure of the ingot, refining the dispersed indium phase inclusions in a macroscopically homogeneous ingot.

Thus, a tendency to macroscopic delamination is suppressed in the alloys of monotectic systems solidified from the melts subjected to preliminary HHT, which makes it possible to form castings with dispersed indium phase inclusions in a macroscopically homogeneous ingot.

Commercial Aluminum Alloys

In this section, the wide possibilities for the effective use of heat treatment of a melt to control the structure and properties in a solid state are illustrated by the example of a number of granular and cast alloys.

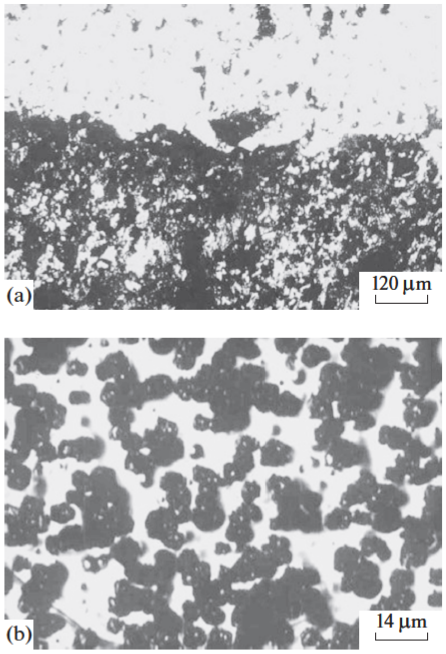

Fig. 20. Structure of the Al–20 at % In alloy solidified at a cooling rate $V = 1$ K/s from temperatures (a) inside the metastable microheterogeneity region (overheating $\Delta T = 70$ K above liquidus) and (b) outside this region ($\Delta T = 600$ K).

The heat resistance of Al–Zr–Cr alloys is known to be provided by refractory additives, which precipitate in the form of dispersed intermetallic compounds during the processing of granules or ribbons into semifinished products. The technology for the production of semifinished products from granular alloys requires a homogeneous fine as-cast structure. However, this problem is complicated by the presence of primary aluminide crystals in the as-cast structure. Their presence, which sharply worsens the mechanical properties of the alloys, is responsible for the low stability of transition metals in aluminum. The most traditional method for their elimination is the use of technologies for the production of ribbons or powders in which the cooling rate during quenching from a liquid state reaches 10^4 K/s or more

In our experiment, for the same purpose we used heat treatment of initial melts as an alternative to their rapid quenching. The homogenization temperatures of ternary Al–Zr–Cr alloys with a transition metal content below 4.5% were found to lie between 1230 and 1250°C.

The appearance of the metastable Al_3Zr modification in the ternary alloys was found under the same

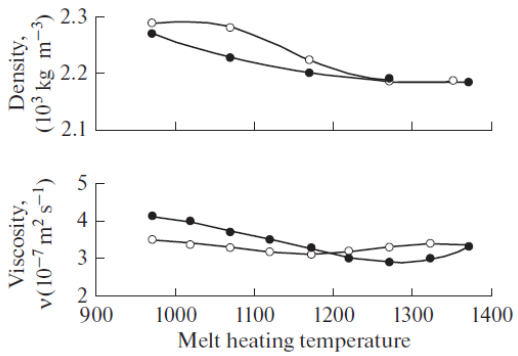

Fig. 21. Temperature dependences of the kinematic viscosity (ν) and density (*d*) of an Al9 alloy in the liquid state: (●) heating and (○) cooling.

conditions as in binary Al–Zr analogs. As the melt overheating increases, rounded cubic growth shapes are replaced by dendritic forms, which differ in the anisotropy of the growth rates of secondary dendrite arms. Preliminary heating of a melt to the temperature close to the homogenization temperature sharply increases the number of aluminides and decreases their sizes. As a result, a dispersed, about 5 μm in size, subdendritic structure of the α solid solution forms. When the melt temperature exceeded T_{hom}, stable growth of dispersed metastable Al_3Zr aluminides was observed in the as-cast structure of the Al–3Zr–1Cr alloy (wt %). When the melt temperature increases, the α solid solution is additionally alloyed with zirconium (up to 0.25–0.3%), which is accompanied by an increase in its microhardness by 20 MPa.

Summarizing these experimental results, we can conclude that the following two heat treatment schedules can be used for a melt to improve the structure of granular heat-resistant Al–Cr–Zr alloys.

The first schedule with $T > T_{hom}$ makes it possible to suppress the primary solidification of aluminides and to form the structure of an anomalously supersaturated α solid solution at moderate cooling rates. An increase in the alloying of the solid solution increases its thermal stability and improves its mechanical properties to $\sigma_u = 380$ MPa, $\sigma_{0.2} = 340$ MPa, and $\delta = 12\%$.

The second schedule, where a melt is heated slightly below $T_{hom,}$ ensures the formation of dispersed crystals of the metastable Al_3Zr phase and a subdendritic structure of the α solid solution. Such a structure is additionally hardened in comparison with nonoverheated samples, especially in the cases where the zirconium content exceeds the zirconium solubility limit (at a given cooling rate).

Silumins, i.e., Al–Si alloys are used in the manufacture of castings with high service properties, such as air-tightness, corrosion resistance, and strength. A typical representative of this class of alloys is an Al9 alloy with an almost eutectic composition and a high strength due to alloying with magnesium. However, the use of this alloy for the production of castings of a complex geometric shape requires an increase in the ductility at the same level of strength properties.

We proposed heat treatment of the alloy melt for this purpose. The melt heating conditions were chosen using the measured temperature dependences of the density and viscosity. The data presented in Fig. 21 confirm the fact that this melt is a complex microheterogeneous system, which retains a metastable state at least up to 950°C [40].

An increase in the casting temperature is shown to suppress the formation of large needle-shaped silicon crystals and is accompanied by refining the main structural constituents, namely, eutectic and α solid solution. When the temperature of primary heating of the melt increases, the microhardness of the α-solid solution dendrites in the as-cast state increases from 580 to 710 MPa and the relative elongation increases. The ultimate tensile strength σ_u is less sensitive to changes in this temperature. If the maximum melt heating temperature was below T_{hom}, these effects were not preserved during subsequent cooling to the casting temperature (720°C in our experiments). Nevertheless, the values of δ are twice as high as the values measured after a standard technology without heat treatment of the initial melt.

Alternative results were obtained after overheating of the melt above the homogenization temperature. This heat treatment was found to retain high values of σ_u and δ even at low casting temperatures.

These results proved the usefulness of heat treatment of melts as a technological tool for improving the properties and quality of commercial aluminum alloys

CONCLUSIONS

In this article, we tried to show that liquid metals are very complex systems. They can change their structural state under the influence of temperature variation or other external actions. On the other hand, the characteristic features of the initial melt can be retained in solidified samples as a result of its cooling at a proper rate. As a result, the structure and properties of solidified alloys can be controlled by adjusting the melting and solidification conditions. The examples presented here indicate the high efficiency of heat treatment of initial melts to improve the structure and properties of aluminum alloys with various types of phase diagrams.

REFERENCES

1. B. A. Baum, G. A. Khasin, and G. V. Tyagunov, *Liquid Steel* (Metallurgiya, Moscow, 1984).
2. G. V. Tyagunov, E. E. Baryshev, V. S. Tsepelev, et al., *Metallic Liquids. Steels and Alloys* (UrFU, Yekaterinburg, 2016).
3. I. G. Brodova, P. S. Popel, and G. I. Eskin, *Liquid Metal Processing: Application to Aluminium Alloy Production* (Taylor & Francis, London, 2001).
4. V. Manov, P. Popel, E. Brook-Levinson, et al., "Influence of the thermal treatment of melt on the properties of amorphous materials: ribbons, bulks and glass coated microwires," Mater. Sci. Eng. A **A304–306**, 3–54 (2001).
5. A. C. Mitus and A. Z. Patashinsky, "A statistical description of local structure of condensed matter," Physica A **150**, 383–391 (1988).
6. A. Z. Patashinsky and B. I. Shumilo, "Theory of condensed matter based on the hypothesis of local crystalline order," Zh. Eksp. Teor. Fiz. **89** (1), 315–328 (1985).
7. L. D. Son, "Statistical models of structure and transitions in liquid," Doctoral Dissertation in Mathematics and Physics (Yekaterinburg, 2007).
8. A. C. Mitus and A. Z. Patashinsky, "Cluster model of melting and premelting of metals," Sov. Phys. JETP **53**, 798–801 (1981).
9. A. C. Mitus and A. Z. Patashinsky, "The theory of crystal ordering," Phys. Lett. A **87**, 179–182 (1982).
10. V. E. Sidorov, L. D. Son, G. M. Rusakov, and B. A. Baum, "The peculiarities in crystallization of iron containing 2.0 wt % of carbon," High Temp. Mater. Proc. **14** (4), 263–271 (1995).
11. G. M. Rusakov, L. D. Son, L. I. Leont'ev, and K. Yu. Shunyaev, "Liquids–liquids structural transition in a system with an impurity," Dokl. Akad. Nauk **411** (4), 467–471 (2006).
12. O. I. Ostrovskii, V. A. Grigoryan, and A. F. Vishkarev, *Properties of Metallic Melts* (Metallurgiya, Moscow, 1988).
13. V. E. Sidorov, V. S. Gushchin, and B. A. Baum, "Magnetic structure of iron containing oxygen," Phys. Status Solidi A **85**, 497–501 (1984).
14. E. A. Klimenkov, P. V. Gel'd, B. A. Baum, and Ju. A. Bazin, "On the short range in liquid iron, cobalt and nickel," Dokl. Akad. Nauk SSSR **230**, 71 (1977).
15. L. D. Son and V. E. Sidorov, "Polymerization in glass-forming melts," Izv. Akad. Nauk, Ser. Fiz. **65** (10), 1402 (2001).
16. R. Kumar and C. S. Sivaramakrishnan, "Stability of liquid Pb–Cd systems," J. Mater. Sci. **5** (4), 377–382 (1969).
17. I. V. Gavrilin, "Sedimentational experiment for studying liquid alloys," Izv. Akad. Nauk SSSR, Ser. Met., No. 2, 66–73 (1985).
18. P. S. Popel, O. A. Chikova, and V. M. Matveev, "Metastable colloidal states of liquid metallic solutions," High. Temp. Mater. Proc. **4** (4), 219–233 (1995).
19. P. S. Popel and V. E. Sidorov, "Microheterogeneity of liquid metallic solutions and its influence on the structure and properties of rapidly quenched alloys," Mater. Sci. Eng. A 226–228, 237–244 (1997).
20. B. P. Gol'tyakov, P. S. Popel', V. Ya. Prokhorenko, and V. E. Sidorov, "Magnetic effects confirming metastable microheterogeneity of Au–Co melts," Rasplavy **2**, (6), 83–86 (1988).
21. P. S. Popel', V. P. Manov, and A. B. Manukhin, "Influence of the state of melt on the structure of Sn–Pb films after solidification," Dokl. Akad. Nauk SSSR **281** (1), 107–109 (1985).
22. U. Dahlborg, M. Calvo-Dahlborg, P. S. Popel', and V. E. Sidorov, "Structure and properties of some glass-forming liquid alloys," Eur. Phys. J. B **14**, 639–648 (2000).
23. V. V. Makeev and P. S. Popel', "Volume characteristics of Ni–B alloys in the range from 1100 to 2170 K," Zh. Fiz. Khim. **64**, 568–572 (1990).
24. U. Dahlborg, J.-G. Gasser, G. J. Cuello, S. Mehraban, N. Lavery, and M. Calvo-Dahlborg, "Temperature and time dependent structure of the molten Ni81P19 alloy by neutron diffraction," J. Non- Cryst Solids **500**, 359–365 (2018).
25. S. N. Kuzin and P. S. Popel, "Gas bubbles in melts and their role in metal porosity formation," in *Proceedings of 5th Conference on Heredity in Cast Alloys* (SamGTU, Samara, 1993), pp. 116–119.
26. V. M. Matveev, P. S. Popel', and O. A. Chikova, "Influence of Mg, Gd, Zn, Cd, Zr, Sc, B, Ti, and Mn additions on the thermal stability of the microheterogeneous state of the Al–5.4 at % Sn melts," Rasplavy, No. 2, 82–86 (1995).
27. P. S. Popel, V. I. Nikitin, I. G. Brodova, et al., "Influence of the structural state of melt on the solidification of silumins," Rasplavy **1** (3), 31–35 (1987).
28. P. S. Popel', O. A. Korzhavina, I. G. Brodova, et al., "Viscosity and electrical resistivity of the Al–Si melts and the influence of their structural state on the structure of cast metal," Rasplavy, No. 1, 10–17 (1991).
29. N. Yu. Konstantinova, P. S. Popel', and D. A. Yagodin, "Kinematic viscosity of liquid copper–aluminum alloys," TVT **47** (3), 354–359 (2009).
30. A. R. Kurochkin, P. S. Popel', A. V. Borisenko, and D. A. Yagodin, "Divergence of temperature dependences of gamma-ray beam attenuation in the penetrated zone of Cu–Al melts at heating and subsequent cooling," High Temp.-High Pres. **44** (4), 265–283 (2015).
31. V. V. Astaf'ev, A. R. Kurochkin, N. I. Yablonskikh, et al., "Influence of homogenizing heat treatment of liquid aluminum–copper alloys on the structure of rapidly quenched samples," Metalloved. Term. Obrab. Met., No. 8, 20–23 (2017).
32. I. G. Brodova, V. M. Zamyatin, and P. S. Popel', "Conditions for the formation of metastable phases during the solidification of the Al–Zr melts," Rasplavy **2** (6), 83–86 (1988).
33. I. G. Brodova, L. V. Bashlykov, I. V. Polents, and O. A. Chikova, "Influence of heat melt treatment on

the structure and the properties of rapidly solidified aluminum alloys with transition metals," Mater. Sci. Eng. A **226–228**, 136–140 (1997).

34. I. G. Brodova, I. V. Polents, L. V. Bashlykov, et al., "The forming mechanism of ultradispersed phases in rapidly solidified aluminum alloys," Nanostr. Mater. **6** (1–4), 477–479 (1995).
35. R. E. Ryltcev and L. D. Son, "Statistical description of glass-forming alloys with chemical interaction: application to Al–R systems," Physica B, No. 406, 3625–3630 (2011).
36. I. I. Ivanov, V. C. Zemskaya, V. K. Kubasov, et al., *Melting, solidification, and shape formation at Low Gravity* (Nauka, Moscow, 1979).
37. V. I. Dobatkin and V. I. Elagin, *Granulated Aluminum Alloys* (Metallurgiya, Moscow, 1981).
38. P. S. Popel', O. A. Chikova, I. G. Brodova, and I. V. Polents, "Structure formation during the solidification of Al–In alloys," Fiz. Met. Metalloved., No. 9, 111–115 (1992).
39. L. A. Zhukova and S. I. Popel', "Electron diffraction study of the structure of melts," Zh. Fiz. Khim. **56** (11), 2702 (1982).
40. J. Hohler and J. Steeb, "Struktur von aluminium–indium schmelzen mittels rontgenweitwinkelbeugung," Z. Naturforsch. A **30** (6–7), 771–774 (1975).
41. G. I. Batalin, E. A. Beloborodova, and V. P. Kazimirov, *Thermodynamics and Structure of Liquid Aluminum-Based Alloys* (Metallurgiya, Moscow, 1983).

Translated by K. Shakhlevich